Systemic seismic risk assessment of road networks considering interactions with the built environment

Sotirios Argyroudis*,

Department of Civil Engineering, Aristotle University of Thessaloniki, POB 424, 54124, Thessaloniki, Greece

Jacopo Selva,

Istituto Nazionale di Geofisica e Vulcanologia, via D. Creti 12, 40128, Bologna

Pierre Gehl,

BRGM, 3 avenue Claude Guillemin, BP36009, 45060 Orleans Cedex 2, France

&

Kyriazis Pitilakis,

Department of Civil Engineering, Aristotle University of Thessaloniki, POB 424, 54124, Thessaloniki, Greece

Abstract: *This paper presents an integrated approach for the probabilistic systemic risk analysis of a road network considering spatial seismic hazard with correlation of ground motion intensities, vulnerability of the network components, and the effect of interactions within the network, as well as, between roadway components and built environment to the network functionality. The system performance is evaluated at the system level through a global connectivity performance indicator, which depends on both physical damages to its components and induced functionality losses due to interactions with other systems. An object-oriented modeling paradigm is used, where the complex problem of several interacting systems is decomposed in a number of interacting objects, accounting for intra- and inter-dependencies between and within systems. Each system is specified with its components, solving algorithms, performance indicators and interactions with other systems. The proposed approach is implemented for the analysis of the road network in the city of Thessaloniki (Greece) in order to demonstrate its applicability. In particular, the risk for the road network in the area is calculated, specifically focusing on the short-term impact of seismic events (just after the earthquake). The potential of road blockages due to collapses of adjacent buildings and overpass bridges is analyzed, trying to individuate possible criticalities related to specific components/sub-systems. The application can be extended based on the proposed approach, to account for other interactions such as failure of pipelines beneath the road segments, collapse of adjacent electric poles or malfunction of lighting and signaling systems due to damage in the electric power network.*

1 INTRODUCTION

The experience of past earthquakes reveals that roadway elements are quite vulnerable and their damage could be greatly disruptive due to the lack of redundancy, the lengthy repair time or the rerouting difficulties. The traffic disruption can strongly affect the emergency and rescue operations immediately after the earthquake as well as the reconstruction effort and other activities in the following period. Examples of damages to urban or regional road

networks that resulted to short- and long- term impacts can be found in several earthquakes: 1994 Northridge, USA (Perkins et al., 1997); 1995 Kobe and 2004 Niigata ken Chuetsu, Japan (NIST, 1996; Bardet, 2004); 2008 Wenchuan, China (Tang et al., 2011); 2009 L'Aquila, Italy (Dolce et al., 2009) and others. The complexity of network components, their variability from one place and one country to another, the spatial variability of ground motion and until recently, the lack of well validated damage and loss data from strong earthquakes, have made the vulnerability assessment of each particular component, and of the network as a whole, a quite challenging issue. This task is further complicated by the spatial extent of transportation networks, the interactions with other systems and the inherent epistemic and aleatory uncertainties in all the steps toward the risk assessment (e.g., in seismic hazard, fragility, functionality and loss modeling according to Pate-Cornell, 1996; Woo, 1999; Selva et al., 2013, among others).

Several studies have been published proposing and applying methodologies for the seismic risk assessment of transportation systems. They can be distinguished according to the time frame considered (emergency phase or economic recovery phase), the scale (urban, regional, national) and the needs of stakeholders (emergency planning, mitigation or network extension planning, insurance). Generally speaking, they can be classified in three levels: connectivity, capacity and integrated loss estimation. In connectivity analyses, the attention is given on the integrity of the network. They focus on one of the services provided by the network, e.g., most typically the rescue function immediately after the earthquake, and they may be of interest in identifying portions of the network that are critical with respect to its continued connectivity (Nuti and Vanzi, 1998; Goretti and Sarli, 2006; Franchin et al., 2006). In capacity analysis, the scope is widened to include consideration of the network capability to accommodate traffic flows. The increase of travel time in the damaged network is estimated and sometimes translated into monetary terms. This indirect loss summed with direct losses due to physical damages, results in a first partial estimate of the overall economic impact of an earthquake (Kiremidjian et al., 2007; Chang et al., 2011). The effect of retrofitting strategies and restoration works in the performance of the network is considered in some cases (Werner et al., 2000; Zhou et al., 2004). Integrated analyses aim at obtaining a realistic estimate of total loss, inclusive of direct physical damage to structures (residential and industrial buildings as well as network components), loss due to reduced activity in the economic sectors (industry, services), and network-related loss (increased travel time). Economic interdependencies are accounted for, such as the reduction in demand and supply of commodities (due to damaged factories, etc.), which, coupled to increased travel costs, may lead to reductions in the demand for travel. At this level the relevance and the complexity of the economic models become dominant over that of the transportation network (Cho et al., 2001; Veneziano et al., 2002; Karaca, 2005).

All the methods mentioned above are based on different simplifications and/or assumptions that introduce numerous uncertainties. The most critical aspects are related to the hazard characterization and the treatment of interactions among different systems. Hazard characterization for spatially extended infrastructures is particularly challenging, since spatial correlations and spatial cross-correlations of ground motion intensities may play an important role (Crowley et al., 2008; Esposito and Iervolino, 2011). Indeed, the use of aggregated hazard assessments (in which the effects of all the possible sources are aggregated together) may introduce uncontrolled biases in the analysis, especially when interconnected components or networks are analyzed (Adachi, 2007; Adachi and Ellingwood, 2009). In addition to this, different components may have fragility models expressed with different intensity measures, implying the necessity of evaluating an entire set of statistically correlated intensity measures. As regards the interaction among systems, the effect of 'external' systems influencing the functionality of system components, independently of their physical state, may introduce additional failure modes that are often completely neglected. Furthermore, the variety of analysis techniques, seismic hazard and damage models being used, strongly influence the derived estimates, producing significant discrepancies between the seismic risk assessments made by different authorities for the same location and structure type (see discussion in Selva et al., 2013).

Within the recent SYNER-G project, funded by the European Commission (SYNER-G, 2013), a general methodology has been developed for the seismic vulnerability assessment of an infrastructure of urban/regional extension, accounting for inter- and intra-dependencies among infrastructural components, as well as for the uncertainties characterizing the problem. More specifically, models of the infrastructure and of the hazard acting upon it have been set up, and the analysis methods that evaluate the system performance accounting for a large set of uncertainties were introduced (Franchin, 2013). In this general framework, also some socio-economic consequences can be assessed, analyzing shelter needs and health care impact. Probabilistic evaluation of the performance of networks is carried out by means of Monte Carlo simulations. This general framework can be adopted at the different levels of systemic analyses described above. In order to tackle the complexity of the described problem the object-oriented paradigm (OOP) has been adopted. In abstract terms, within such a paradigm, the problem is described as a set of classes, characterized in terms of attributes and methods, interacting with each other (Franchin and Cavalieri, 2013). Objects are instances

(concrete realizations) of the classes (abstract models, or templates for all objects with the same set of properties and methods).

This general framework may find application to many different analyses, with different statistical approaches, target networks, and scopes (e.g., Cavalieri et al., 2012; Esposito et al., 2014). The application of this general methodology is essentially based on two steps: (i) the seismic hazard characterization through realizations of ground motions and (ii) the probabilistic evaluation of the target system's performance conditional on such realizations. In particular, the development of the hazard model has the goal of providing a tool for: a) sampling events in terms of location (epicentre), magnitude and faulting style according to the seismicity of the study region and b) maps of sampled correlated seismic intensities at the sites of the vulnerable components in the infrastructure ('shakefields' method, see Section 2.1). These maps, conditional on the occurrence of one earthquake with given magnitude and hypocenter are meant to realistically describe the variability and spatial correlation of intensity measures at different sites, which is a fundamental request for the analysis of spatially extended networks (e.g., Adachi, 2007). Further, when more vulnerable components exist at the same location and their fragility is expressed with different intensity measures (e.g., peak ground acceleration and displacement), the model assesses them in a consistent way (under specific hypotheses, see discussion in Weatherill et al., 2014). The development of the physical model for the network starts from the SYNER-G taxonomy and requires: a) for each system within the taxonomy, a description of the functioning of the system (intra-system dependencies) under both undisturbed and disturbed conditions (i.e., in the damaged state following an earthquake); b) a model for the physical and functional (seismic) damageability of each component within each system (fragility functions); c) identification of all dependencies between the systems (inter-dependencies); and d) definition of adequate Performance Indicators (PIs) for components and systems, and for the infrastructure as a whole (Franchin, 2013).

This paper is focused on the implementation of this general framework to road network analysis. For simplicity, a pure connectivity analysis is adopted, and the problem of interaction between the road network and the built environment is specifically addressed. The computational modules include the following main models: the hazard class that models the earthquake events and corresponding seismic intensity parameters; the road network class that models the physical damages of the network components and the overall system's performance; the inderdependencies models that simulate the buildings' damages and the induced debris due to collapses as well as the road blockage due to collapsed buildings and due to collapsed bridges. The strength of such interactions is evaluated by quantifying their effects on risk curve, that is, mean annual rates of exceedance for loss in performance of the network, as measured by appropriate PIs. The correlation between single components (either internal or external to the system) and global performance is also analyzed, in order to evaluate possible strategies for risk reduction actions. For simplicity, focus is given on the performance in the aftermath of seismic events; therefore the results can be used as a basis for the implementation of long term mitigation planning. The computational framework is demonstrated and tested through an application to the main road network of city of Thessaloniki in Greece.

2 ROADWAY NETWORK ANALYSIS

The goal of the analysis is to evaluate probabilities or mean annual rates of events E defined in terms of network performance indicators. This requires the assessment of a joint probability model accounting for inherent uncertainties. The joint pdf (probability density function), $f(x)$, can be written as a product of a set of conditional distributions in the following form (Franchin, 2013; Cavalieri et al., 2012):

$$f(\boldsymbol{x}) = f_{SYS|PhVM}(\boldsymbol{x}_{SYS}|\boldsymbol{x}_{PhVM}) f_{PhVM|SH}(\boldsymbol{x}_{PhVM}|\boldsymbol{x}_{SH}) f_{SH}(\boldsymbol{x}_{SH}) \quad (1)$$

where x is the vector that collects the random variables in seismic hazard (SH), physical vulnerability model (PhVM) and systemic analysis model (SYS). Equation 1 highlights the statistical dependencies between the variables, also specifying the sampling sequence within a directed acyclic graph (DAG) that goes from seismic hazard up to the systemic analysis (for more details, see Franchin, 2013). The probabilistic terms are asssessed under the assumption of uni-directional physical dependencies among the different steps of the analysis. This means, for example, that system failures cannot affect backward single components performance. Here, for simplicity, uncertainty on the functional form and on the parameters of each distribution $f(.)$ is not considered, that is, epistemic uncertainty on probabilistic models is neglected. Thus, the focus is on the assessment of each term of $f(.)$, which describe the inherent aleatory uncertainties. In particular, the term f_{SH} includes the spatio-temporal occurrence of earthquakes, attenuation models, spatial correlations for each intensity measure, and cross-correlations among different intensities. The term $f_{PhCM|SH}$ essentially includes the fragility of all the components of all the systems. The term $f_{SYS|PhVM}$ includes the systemic model for all the analyzed systems, and it considers functional consequences of physical damages, as well as inter- and intra- dependencies among components and systems. The functional implementation of these terms is discussed in Section 3.

The final goal of the assessment is the marginal distribution of $f(\mathbf{x})$, with respect to all the hazard ($\mathbf{x}_{SH}$) and vulnerability ($\mathbf{x}_{PhVM}$) variables, describing the exceedance probability of different levels of performance for the systems under the effect of any possible seismic input and physical damages. This output, hereinafter referred to as performance curve, is the equivalent of risk curves for non-systemic probabilistic assessments in single (e.g., Pacific Earthquake Engineering Research PEER formula, Cornell and Krawinkler, 2000) and/or multi-risk (e.g., Grunthal et al., 2006; Selva, 2013) analysis. The analysis of this marginal distribution is here carried out based on a Monte Carlo simulation-based method. This approach, with respect to other non-sampling-based approaches (e.g., Song and Ok, 2010; Duenas-Osorio and Rojo, 2010), facilitates the implementation of different levels of network analysis, also including inter- and intra-network dependencies, and it allows considering complex inhomogeneous networks, within a modelling environment which is easily controlled and interpretable (Cavalieri et al., 2012).

In the following subsections, the specific implementations regarding the road network (RDN) analysis are described. The network is specified in terms of:

- Taxonomy of the components within the network and associated vulnerability.
- Solving algorithms used to assess the network's performance.
- Nature of the interactions with components from other systems (i.e., interdependencies).

2.1 Taxonomy of the network

Taxonomy and typology are fundamental elements in seismic risk assessments. They describe the morphology of the network and the features that are critical for the seismic response of each component. The road network is composed of a number of nodes and edges, which are vulnerable to seismic shaking or ground failures due to geotechnical hazards such as liquefaction, landslides and fault rupture. The main element is the road itself, which is passing over or under bridges, through tunnels or on embankments and other civil works. Therefore the hierarchy of roads according to their functions and capacities is an important parameter for the description of the typology. Several classification systems have been proposed for each network and component. In the context of SYNER-G project a new taxonomy has been proposed which identify the main typologies of the networks (Hancilar and Taucer, 2013). The components considered in the present work are the followings:

- Bridges: The main features used to describe a bridge, comprise the material, type and structural system of the deck, type of piers and their connection to the deck, number of spans and length, type of connection to the abutments, skew, regularity, type of foundation and level of seismic design (Tsionis and Fardis, 2014).
- Tunnels: the basic typological parameters are the construction method (bored or mined, cut-and-cover, immersed), the shape (circular, rectangular, horseshoe, etc.), the depth (surface, shallow, deep), the geological conditions (rock, alluvial), and the supporting system (concrete, masonry, steel, etc.).
- Embankments (road on), cuts (road in) and unstable slopes (road on, or running along): the main typological features are the geometrical parameters of the construction (i.e., slope angle, height) and the soil type of the earth structure and surrounding material.
- Road pavements: they described by the number of traffic lanes, which is based on the functional hierarchy of the network.
- Bridge abutments: the main features are the depth and the soil conditions of foundation and fill material behind the abutment.

Most of the elements are classified as edges, however an element is classified as a node when its spatial extension is sufficiently limited (e.g., single span bridge, bridge abutment).

The vulnerability of each element at risk is assessed through fragility curves, which describe the probability that a structure will reach or exceed a certain damage state for a given ground motion intensity (e.g., FEMA, 2003). Fragility curves are usually provided for each typology of structures, assuming that structures with similar characteristics are expected to perform in the same way for a given seismic excitation. Numerous fragility models have been proposed for bridges based on statistical data from recent earthquakes or analytical approaches, which adopt simple or advanced numerical models (e.g., Banerjee and Shinozuka, 2007; Tsionis and Fardis, 2014). The existing fragility functions for the other elements are generally limited and they are mainly based on empirical data or expert judgment approaches (e.g., FEMA, 2003; Werner et al., 2006). Recently, fragility curve derivation methods using numerical approaches have become more widely adopted, as they are readily applicable to different structural types and geographical regions where damage records are insufficient. When necessary, the effect of geotechnical conditions to the fragility of some components such as tunnels, embankments or bridge abutments, is taken into account through numerical modelling of soil-structure-interaction. A brief presentation of existing and recently developed fragility functions for road elements is made by Argyroudis and Kaynia (2014). Another important issue is the effect of corrosion on the seismic response of aging structures as well as the effect of cumulative damages to the physical vulnerability of structures during the aftershock sequences. Recently, these effects have been considered in the fragility assessment of buildings (Pitilakis et al., 2014) and bridges (Ghosh and Padgett, 2010; Franchin and Pinto, 2009), however they are not addressed in the present framework.

2.2 System performance indicators

The performance of the road network under seismic conditions is measured through PIs, which vary depending on the type of analysis (see Section 1). A summary of available performance indicators is given by Modaressi et al. (2014). In the present study a connectivity analysis is performed and the following two PIs are applied:

- *Simple Connectivity Loss, or SCL* (Poljanšek et al., 2012).

It is based on the concept of connectivity, providing a general measure of the average reduction in the ability of sinks to receive flow from sources. The region of interest is divided in Traffic Analysis Zones (TAZs), which represent the origin-destination pairs for the connectivity analysis. In particular, SCL is defined as:

$$SCL = 1 - < \frac{N_s^i}{N_o^i} >_i \quad (2)$$

where < > denotes averaging over all sink vertices, N_s^i and N_o^i are the number of sources connected to the i[th] sink in seismic and non-seismic conditions, respectively. With reference to a RDN, all the single TAZs, taken one at a time, are considered sinks, whereas all the remaining TAZs are sources.

- *Weighted Connectivity Loss, or WCL* (Franchin and Cavalieri, 2013).

This index upgrades the simple connectivity loss by weighting the number of sources connected to the i[th] sink, in seismic and non-seismic conditions:

$$WCL = 1 - < \frac{N_s^i W_s^i}{N_o^i W_o^i} >_i \quad (3)$$

where the weights W_s^i and W_o^i can be defined in different ways, a weighted average can be used as follows:

$$W^i = \sum_{j, j \neq i} I_{ij} \cdot \frac{1}{TT_{ij}} \quad (4)$$

where I_{ij} is equal to 1 when a path exists between the i[th] and the j[th] source, and to 0 otherwise. TT_{ij} is the travel time of the path between the i[th] sink and the j[th] source, it can be evaluated based on the average travel speed considered along the road type and the edge length.

2.3 Interdependencies

Several classifications have been presented to categorize the types of dependencies between systems (e.g., Rinaldi et al., 2001; Dudenhoeffer and Permann, 2006). In the case of road network three general categories are recognized in relation with the earthquake event:

- Physical interactions, associated with the physical reliance on roadway capacity to other networks and services. Damage to road network can block access to: damaged buildings, thus preventing rescue missions; harbour, airport, railway or bus terminals preventing transportation of people and goods; health-care and other critical facilities hindering emergency response.
- Geographic interactions, when the physical proximity of the local environment affects the functionality of the road network. Collapse of adjacent buildings produces debris that can cause road blockages; damage to underground tunnels, water or gas pipelines, adjacent electric power poles or overpass bridges can disrupt the traffic; debris flow due to landslides and rock falls can produce road blockages.
- Demand interactions, which correspond to the generation of travel demand from different user types: demand for emergency vehicles originated from hospitals, fire or police stations and from citizens, demand for transportation of goods and people from harbour, railway or airport terminals.

In the present study the geographic interactions due to collapsed buildings and overpass bridges are considered.

3 IMPLEMENTATION OF THE MODEL AND PROTOTYPE SOFTWARE

3.1 The hazard class

This class is focused in the assessment of the term f_{SH} in Equation 1. A method entitled 'shakefield' has been established in the general methodology of SYNER-G, which allows for the generation of samples of ground motion fields for both single scenario events, and for stochastically generated sets of events for probabilistic seismic risk analysis (Weatherill et al., 2014). The seismic hazard class is modelled as the composition of three classes: 1) the class which generates earthquakes from seismogenetic sources, 2) the class in which earthquake events in terms of localization and magnitude are instantiated, and 3) the class for evaluation of local intensity values at the sites of vulnerable components, which is obtained following two steps.

First, a scalar random field of a so-called primary Intensity Measure (IM) on rock is sampled, on a regular grid covering the study region, as a function of the sampled magnitude and epicenter location, employing a ground motion prediction equation (GMPE) with inter-event and intra-event error terms or residuals. Note that the choice of primary IM should be also based on the availability of spatial correlation model since, at this stage, spatial correlations are also introduced through the intra-event model error (Weatherill et al., 2014). Then, the primary IM is interpolated to all sites and the secondary IMs are sampled from their distribution conditional on the primary IM value (Iervolino et al., 2010). All values are then amplified on the basis of local soil conditions. A geotechnical hazard model is used to sample geotechnical IMs such as permanent ground deformations for components whose fragility model requires one (e.g., road pavements) (Weatherill et al., 2014).

3.2 The RDN class

This class comprises the different methods that are used to perform the analysis of the physical damages to the system's components (term $f_{PhCM|SH}$ in Equation 1) and the analysis of the system's performance, accounting for intra- and inter-dependencies (term $f_{SYS|PhVM}$ in Equation 1), for the parts concerning RDN. The RDN class is a directed graph (i.e., edges have a specific travelling direction) defined by sub-classes that describe the different types of edges and nodes (Figure 1). Here, the general framework developed within SYNER-G (Franchin and Cavalieri, 2013) is updated by adding all the analyses necessary to model intra- and inter-dependencies.

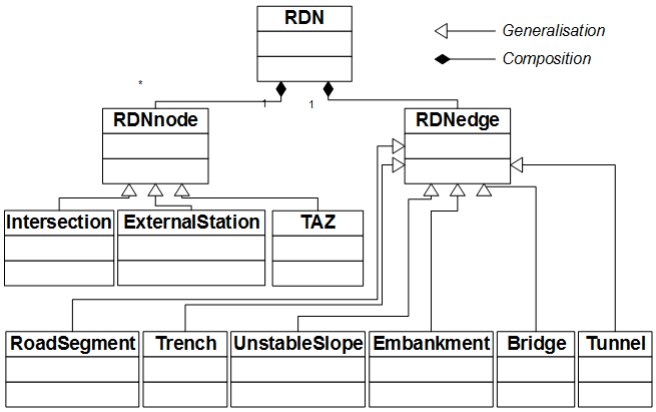

Fig. 1. UML (Unified Modeling Language) class-diagram of the Road Network (RDN)

All the components of RDN are classified within this scheme of abstract sub-classes (RDNnode and RDNedge). Among the types of RDN nodes, *Intersection* nodes simply represent the vertices of the graph that are used to define the edges that can link them: these nodes have no specific properties, except information on coordinates, altitude, soil type and so forth. *TAZ* nodes are nodes that are defined around inhabited areas and they are used to evaluate the connectivity of a given neighborhood to other TAZs (i.e., they are used to build the origin-destination matrix): they have additional properties (such as number of households or the pointer to the inhabited reference cell) that can be used to evaluate traffic demand and connectivity loss for the associated cells. Finally, *ExternalStation* nodes are a type of TAZs that are not associated with the inhabited cells, but they are used to link the studied portion of road network to the 'outside' (i.e., definition of inward/outward traffic demand in the case of an open system).

The types of RDN edges are defined with respect to the physical properties of the road segments (i.e., bridges, tunnels, simple road segments, and roads within a cut, on an embankment or on a slope) and the different vulnerability models that may be used for each one of them (i.e., different damage mechanisms or intensity measures have to be considered for bridges or for a simple road segment). Within each of these edge sub-classes, different typologies are also defined, depending on the material used, the soil type or the construction technique. Some other properties of edges include the pointers to the extremities (i.e., end and start nodes, as the graph is directed), the number of lanes or the number of ways (i.e., in order to generate two directed paths when there are two-ways edges). The definition of edges along with their extremities is used to build an adjacency and an incidence matrix; the former indicates the nodes that an edge is linked to (0 if not linked, 1 otherwise), the latter indicates the direction of the edge with reference to the adjacent nodes. These matrices are used to describe the connectivity of the road network, and subsequently the accessibility of TAZ nodes.

Each physical object is defined as either vulnerable or not vulnerable. When an object is defined vulnerable, a list of IMs is defined and a specific fragility function is associated to each IM. From such fragility functions, physical damages are assessed in order to define the physical state under seismic conditions (term $f_{PhCM|SH}$ in Equation 1). In practice, at this level, for each sampled 'shakefield' (see Section 3.1), physical damages to each vulnerable component are sampled from their specific fragility curves, for all the components considered. Note that this includes both RDN and 'external' components. Indeed, to model the interdependencies with other components/systems, physical damages are also sampled for all the components that may affect RDN. In this paper, the effect of debris from buildings adjacent to RDN is considered, so that physical damages are here sampled also for buildings (see Section 3.3).

Also the system performance is defined within the RDN class (term $f_{SYS|PhVM}$ in Equation 1), and it is assessed with the SCL (Equation 2) and WCL (Equation 3). This assessment is here based on a pure connectivity analysis of functional components under seismic conditions. The functionality of each component depends on (i) the physical damage and their functional consequences, and (ii) the impact on each component of possible damages to other elements (either within RDN or external to it) that may affect the component's functionality. As regards (i), the functionality of each component is simply related to its physical damage (through damage state thresholds). On the contrary, the assessment of (ii) requires the definition of an interaction model. In the next sections, it is reported how this model has been implemented (Section 3.3) and how this affects the overall system performance (Section 3.4).

3.3 Interdependencies models

To account for the interdependencies between RDN and external components/systems, a number of specific implementations are required. In this subsection, the details of such models are reported.

3.3.1 The building class

The building class is composed of an array of cells, which have been generated from an adaptive mesh grid, resulting in the projection of all building-related data (e.g., building typologies, population, utility demand, etc). Building cells are defined with a list of attributes. Parts of them are initial input parameters, which come from databases (e.g., building census, European Urban Audit, land use plan, associated fragility functions); the other ones are related to building damages and losses that are derived based on different methods (physical damage, building usability and habitability, casualties, etc).

Due to issues of data availability and computation capacities, the road network cannot usually be modeled in its smallest levels with the inclusion of minor vicinal roads and streets. Instead, it is common to represent only the highways and other major avenues or main roads. The link between this first-order network and the inhabited cells is then ensured by the creation of a 'dependency edge': it is a virtual road edge that joins each cell centroid to the nearest TAZ, thus materializing the access of the built areas to the entry point of the main road network. It is assumed that this dependency edge can represent the mesh of small streets and roads that connects each building to the main road network. This approach enables to adjust the level of detail of the analyses since it leaves the possibility to model only major roads and to assume that the minor roads may be represented by the virtual dependency edges.

3.3.2 Estimation of collapsed building debris

The volume and extension of debris of collapsed buildings depends on the building geometry (mainly the height) and the type of collapse. The latter depends on the characteristics of the earthquake, the soil conditions, the design of the building (e.g., geometry, structural type), the continuity of building facades and the location of the building within the block. When the building facades are continuous, which is a typical case in areas with densely built-up areas, such as the central parts of most cities in Europe, the buildings are in contact and the collapse direction is bounded in the lateral sides, so the collapse is possible to occur mainly in the front or/and back side of the building. Schweier and Markus (2006) describe collapse mechanisms of RC buildings based on observations from past earthquakes. The most critical types for road blockage are the overturn collapse (related for example with the failure of soil-foundation system due to liquefaction), the debris heaps and the outspread layer collapse.

It is obvious that the estimation of debris extent, which is required for the road blockage assessment, is a complicated problem with many uncertainties; therefore, any attempt requires appropriate engineering judgments and assumptions. In this framework, following Argyroudis (2010), simplified geometrical models are proposed (Figure 2), which correlate the height of buildings *(Y)* with the induced debris width *(W_d)* that is extended further than the initial width of the building *(W)*. These models correspond to collapse in one (models A and B) or two (model C) directions and overturn of the building (model D). Starting from the fact that the volume of the collapsed building *(V_T)* is a fraction *(k_v)* of the original volume *(V_o)*, (i.e., $V_T = k_v V_o$), an equation can be defined for each model, which estimates the debris width *(W_d)*, as a function of *W, c, k_v* and *Y* (Figure 2). The angle *c* describes the inclination of the collapse. Sensitivity analyses show that the factors *c* and k_v are the most important, therefore a constant value of *W* can be considered as representative of the study area (Argyroudis, 2010). To describe the aleatory uncertainty in W_d, we assumed that it follows a normal (Gaussian) distribution, defined by two parameters, the mean value, $E[W_d]$, and the standard deviation, σ_{Wd}. These two parameters can be estimated for given mean values and coefficient of variation of *c* and k_v based on the point estimate method (Harr, 1987). In this way, the exceedance probability of a given W_d can be calculated when the building height is known.

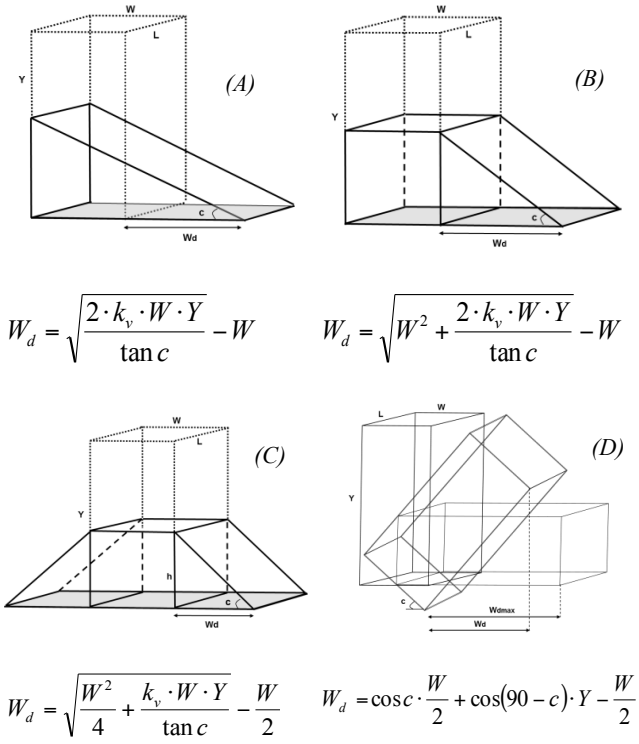

$$W_d = \sqrt{\frac{2 \cdot k_v \cdot W \cdot Y}{\tan c}} - W \qquad W_d = \sqrt{W^2 + \frac{2 \cdot k_v \cdot W \cdot Y}{\tan c}} - W$$

$$W_d = \sqrt{\frac{W^2}{4} + \frac{k_v \cdot W \cdot Y}{\tan c}} - \frac{W}{2} \qquad W_d = \cos c \cdot \frac{W}{2} + \cos(90 - c) \cdot Y - \frac{W}{2}$$

Fig. 2. Estimation of debris width W_d for collapse in one direction (A, B), two directions (C) and overturn (D) (Argyroudis, 2010).

3.3.3 Road blockage due to collapsed buildings

Road network vulnerability in urban areas due to interactions with adjacent buildings has been the object of a few studies in the past. For instance, Goretti and Sarli (2006) propose to sample the number of blockages along a road using a Poisson distribution, as the number of buildings

potentially blocking the road relies on the percentage on built road length and a mean building length. Road blockage due to short-term countermeasures (i.e., propping of damaged facades) is also accounted for. Another study by Tung (2004) introduces a linear density of collapsed buildings, based on the ratio between the area of collapsed buildings and the total area of buildings: a corrective factor is used to account for heterogeneities in the construction pattern. A simplified road blockage model is developed herein maintaining the consistency with the RDN and building classes of the SYNER-G general framework. The main challenge has been to propose a seamlessly integrated approach that makes use of the input attributes that are readily available, without requiring any additional data or parameters. In particular, the road blockage model has been first implemented for dependency edges, because it is assumed that these lower order roads are the most prone to road blockage, due to the narrow streets and to proximity to city buildings. The road blockage model needs the following input attributes for each cell that is crossed by a segment of a dependency edge (see Figure 3):

- A vector $T= [\%T_1 \dots \%T_n]$ giving the repartition of building percentages for the n typologies present in the cell.
- Y, the average building height in the cell. This information could be obtained as a first approximation by the distinction between low-, medium- or high-rise typologies.
- L, the length of the depending edge that is projected in the cell (i.e., distance between the cell centroid and the nearest TAZ). Since buildings can be located on both sides of the road, or not at all, an effective length L' is defined. It is equal to 0, L, or $2L$, depending on the road-building configuration (no buildings, one row of buildings, buildings on both sides, respectively).
- W_r and W_{br}, which are the road width and the building-to-road distance, respectively. These parameters are used in the comparison with the debris width in the eventuality of a building collapsed.
- $1/l$, the linear density of building facade along an edge: this parameter is the key to estimate the number of adjacent buildings along a given edge. A very rough approximation can be given by the following relation, which has the advantage of requiring readily available parameters (i.e., N_b the total number of buildings in the cell and A the area of the cell):

$$\frac{1}{l} = \sqrt{\frac{N_b}{A}} \tag{5}$$

This procedure represents an efficient way to compute the linear density of buildings' edges in a rough approximation: yet, its accuracy depends highly on the shape of buildings and the uniformity of the repartition of buildings in the cell.

For each sampled seismic hazard field, the physical damages to buildings are sampled from specific fragility functions relative to all building typologies within the defined taxonomy ($f_{PhCM|SH}$ in Equation 1 for the buildings). The road blockage model then uses the damage state of each typology within the cell, generating the vector $C=[C_1 \dots C_n]$, which contains the collapse state (0 for not collapsed, 1 for collapsed) for the n typologies present in the cell.

The total number of buildings from typology i that are collapsed along the edge of length L' is then expressed as follows:

$$N_i = \frac{L'}{l} \cdot \%T_i \cdot C_i \tag{6}$$

It has to be noted that a corrective factor should be used to distinguish buildings that are in a complete damage state (as indicated by the fragility analysis) from the ones that are fully collapsed. For the time being, no study or information could lead to an estimation of this corrective factor for the different typologies, and it has been decided as a first approximation to set this factor to 1 (i.e., all N_i buildings are considered as fully collapsed).

Then, the models described in Section 3.3.2 are used to estimate the probabilistic distribution (Gaussian) of the debris width W_d, based on parameters such as building height, typology or collapse behavior. Three functionality levels are defined, assuming a necessary minimum width of 3.5 m for emergency vehicles to go through:

- FL_0, when $W_{d,i} \leq W_{br}$: the edge is 'open';
- FL_1, when $W_{br} < W_{d,i} \leq W_{br} + W_r - 3.5$: the edge is only 'open for emergency';
- FL_2, when $W_{d,i} > W_{br} + W_r - 3.5$: the edge is 'closed';

The use of the effective length L' to model buildings on both sides of the road may present some limitations. For instance, when two buildings have been collapsed at the same place, at both sides of the road, their debris width may not exceed the FL_2 criterion if taken separately; however when they are combined, the remaining free space on the road may become inferior to 3.5 (FL_2 criterion satisfied). Nevertheless, the likelihood of such a configuration may be negligible, especially with respect to the other assumptions developed through the study and to the adopted level of analysis.

The probability of reaching each functionality level of the edge due to each typology, namely $P(FL_{1,i})$ and $P(FL_{2,i})$, can therefore be computed with the knowledge of the distribution parameters, $E[W_d]$ and σ_{Wd}. Finally, the blockage probabilities are aggregated over the length of the edge, by accounting for all typologies of adjacent buildings. Since only one blockage due to one collapsed building is enough to block a road segment, the failure event of the edge can be represented by fault-tree with a succession of *OR* gates corresponding to each collapsed building (i.e., the survival event of the edge is decomposed into a series system of individual survivals to each building collapse). It should be stressed that the individual collapse events are

modelled given the sampled shakefield, that is, one IM value at each cell area. Thus, such collapses can be considered as independent events, except when there is physical connection among the structures (i.e., building aggregates). In general, it is possible to constraint the blockage probability of the edge of length L by the following first-order bounds, which are found in systems of in-series components (Nielson and DesRoches, 2007):

$$\max_{i=1..n}\left[P\left(FL_{j,i} \mid IM\right)\right] \le P_L\left(FL_j \mid IM\right) \le 1-\prod_{i=1}^{n}\left[1-P\left(FL_{j,i} \mid IM\right)\right]^{N_i} \quad (7)$$

In Equation 7, the lower bound corresponds to the case where all events are perfectly correlated, while the upper bound could be assumed if all events were independent. In the present study, even though buildings are assumed to be structurally independent, the collapse probabilities remain conditionally dependent on the level of seismic loading. Due to the difficulty to accurately quantify the correlation factor between the collapse event of two adjacent buildings, the upper bound has been adopted as an approximation of $P_L(FL_j)$, because more conservative (as opposed to the lower bound) estimations are obtained.

A standard uniform variable can then be sampled over the computed probabilities to check the final state of each edge, i.e., FL_0, FL_1 or FL_2.

When applied on dependency edges, this road blockage model gives information on the accessibility between the TAZs and the centroid of the cells. The results are then given at the level of each cell, under the form of an accessibility index with respect to the road network.

In areas with fairly high buildings close to major road segments (e.g., in downtown areas), it has been decided to apply the road blockage model described above to actual edges of the modeled network, and not only to dependency edges. The procedure is the same, except that the computations are now performed at the level of each RDN edge, and not at the cell level (see Figure 3). Input parameters such as W_r, W_{br} or building adjacency must also be defined by the user for each edge (see next Section), and not for each cell. Finally, the functionality results are also given for each edge, becoming 'open', 'open for emergency' or 'closed'.

3.3.4 Road blockage due to collapsed bridges

Within a road network, it is possible to identify numerous locations with overhanging bridges, which could also generate road blockage if an edge is under a collapsed bridge. Therefore it has been decided to implement a blockage model for this specific situation. Two cases are identified:

- Case 1: the bridge above the edge does not belong to the road network class (i.e., it is not modeled in the case-study).

An input parameter has to be added by the user to specify if the edge is under a bridge, and what the bridge typology is. If this is the case, this edge is then associated with a new RDN sub-class, namely *overCrossBridge*, which possess the same vulnerability features of the given bridge typology. The damage state of this bridge is then computed like any other bridge and, if the bridge appears to be in the collapse state, the state of the underlying edge is changed to *blockedByBridge* (Boolean value).

- Case 2: the bridge above the edge is already a part of the road network class and it is itself modeled like an edge.

In this case, first, an intersection algorithm is run over the whole road network in order to locate all edges that are intersected with a bridge-type edge. These edges are then associated with the bridge edges through an edge pointer. During the probabilistic (Monte Carlo) runs, the physical damages are sampled for all network edges, and if the associated bridge edge is in the collapse state, the state of the underlying edge is changed to *blockedByBridge* (Boolean value).

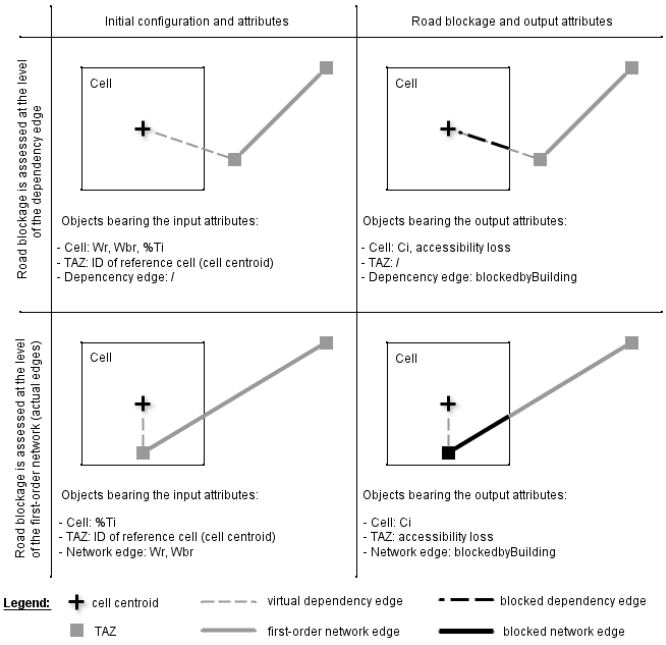

Fig. 3. Schematic view of the two levels of the road blockage model based on the dependency edges in the upper part, on the actual network edges in the lower part.

3.4 Aggregation of functionality losses for connectivity evaluation

As described in the previous sections, RDN edges can be subjected to various disrupting mechanisms from physical failure to interactions with buildings or bridges. These effects may occur at the same time and the following functionality states are defined for each edge during the simulations:

- *Broken*: 0 or 1 (direct physical failure)
- *BlockedbyBuilding*: 'open', 'open for emergency', 'closed'
- *BlockedbyBridge*: 0 or 1

To assess the overall performance of the system (term $f_{SYS|PhVM}$ in Equation 1), these state variables appear in the output attributes of the simulations and they are used to update the adjacency matrix of the RDN class. For each simulation, the values in the adjacency matrix are updated to account for the loss of functionality of some edges (i.e., connectivity analysis). Since here the edge can be disrupted by several causes, the logical tree presented in Figure 4 is adopted to update the adjacency matrix (i.e., use of an OR gate). The updated adjacency matrix is then used to evaluate the connectivity between the different TAZ nodes, which are successively considered as sources or sinks, providing the estimation of the SCL and WCL indicators.

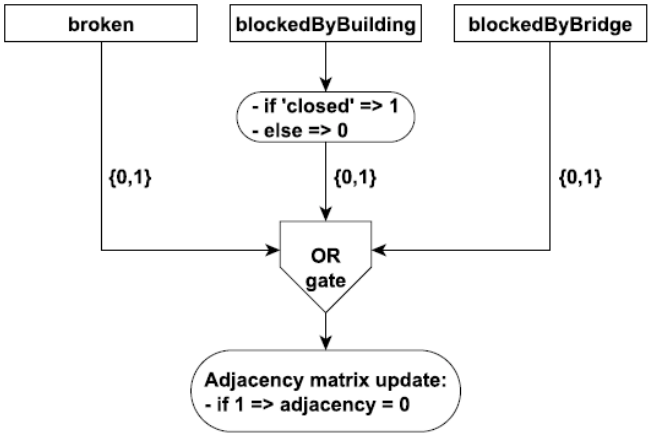

Fig. 4. Update procedure of the adjacency matrix.

4 APPLICATION IN THESSALONIKI

4.1 Seismic hazard

The study area is characterized by intense seismic activity with strong historical earthquakes of magnitudes larger than 6.0. The most recent destructive earthquake occurred in the broader area of Thessaloniki on the Gerakarou-Stivos fault, (20/6/1978, M_w= 6.5). The mainshock caused extensive damage and casualties in the city of Thessaloniki and the surrounding villages (Papazachos and Papazachou, 1997).

For the seismic hazard input of the present application, five seismic zones with M_{min}=5.5 and M_{max}=7.5 are selected based on the results of SHARE European research project (Giardini et al., 2013). The Gutenberg-Richter parameters (a, b) of the zones are given in Table 1. A Monte Carlo simulation (MCS) is carried out sampling seismic events for these zones as described in Section 3.1.

Table 1 Parameters of the seismic zones considered in the case study

Zone	*a*	*b*
GRAS388	4.10	1.00
GRAS390	3.75	0.90
MKAS389	3.90	0.90
MKAS212	4.60	1.00
GRAS392	3.95	1.00

The selected primary IM is peak ground acceleration (PGA) since most of the fragility models used in the analysis are given as a function of this IM. The GMPE introduced by Akkar and Bommer (2010) is applied for the estimation of the ground motion parameters on rock. The spatial variability for PGA is modelled using the correlation models provided by Jayaram and Baker (2009) as adapted for European events consistently with the selected GMPE (Esposito and Iervolino, 2011). For each site of the grid, the averages of primary IM from the specified GMPE were calculated, and the residuals were sampled from a random field of spatially correlated Gaussian variables according to the spatial correlation model.

The primary IM is then retrieved at vulnerable sites by distance-based interpolation and finally the local IM is sampled conditionally on primary IM. Figure 5 shows an example map with the primary IM (PGA at rock) computed at points of a regular grid (3.5 x 4.2 km), for a sampled event with M= 6.0 and R= 12 km. To scale the hazard to the site condition the amplification factors proposed in EC8 (2004) are used in accordance with the site classes that were defined in the study area (i.e., A, B, C classes, Figure 6).

The liquefaction susceptibility of the study area is defined based on the classification scheme introduced by Youd and Perkins (1978), which is adopted in HAZUS (FEMA, 2003) methodology. The classes are categorized on the basis of deposit type, age and general distribution of cohesionless loose sediments (Figure 7). The landslide hazard is not considered in the present case study, as the landslide susceptibility in the study area is very low. The permanent ground deformations, PGD, due to liquefaction are estimated at the vulnerable sites based on the approach of HAZUS and the modelling procedure by Weatherill et al. (2014).

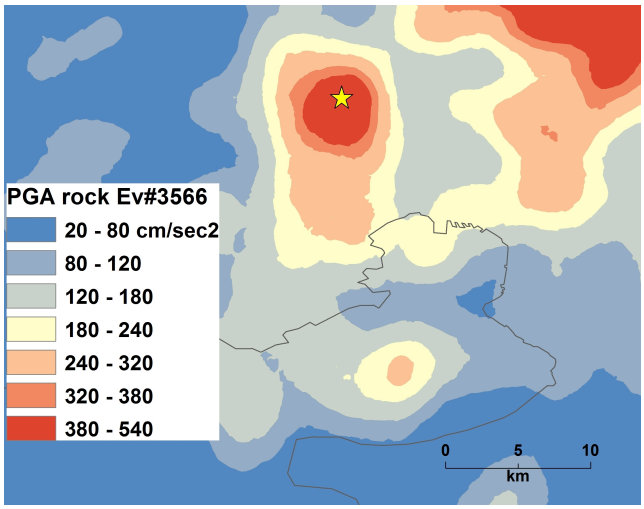

Fig. 5. Example of shake map in terms of PGA on rock for the event#3566 (M=6.0, R=12km).

4.2 System topology and characteristics

The roadway network of Thessaloniki urban area is rather insufficient, especially in the centre districts, where the densely built up area creates a complex network, with narrow streets and inadequate parking space that leads to significant reduction of the effective width of roads due to parked cars. In the present application the main network of the urban area is considered together with the ring road and the main exits of the city where the majority of bridges and overpasses are located. The road network is composed of 594 nodes and 674 edges, which is considered adequate for the needs of this demonstrative application (Figure 8). The required information for the analysis, related to localization, site properties, functionality and vulnerability are given through input workbooks. Site properties such as liquefaction susceptibility and site class are read from the corresponding maps (provided in GIS format). The cell size (for the analysis of buildings) is computed based on the total analyzed area, which includes all the considered components. In this application the cell dimensions are approximately 800 x 800 m.

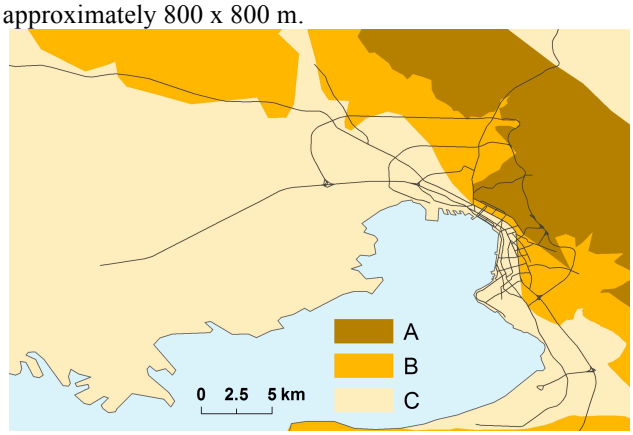

Fig. 6. Simplified geotechnical classification of the study area according to EC8 (based on Pitilakis et al., 2013)

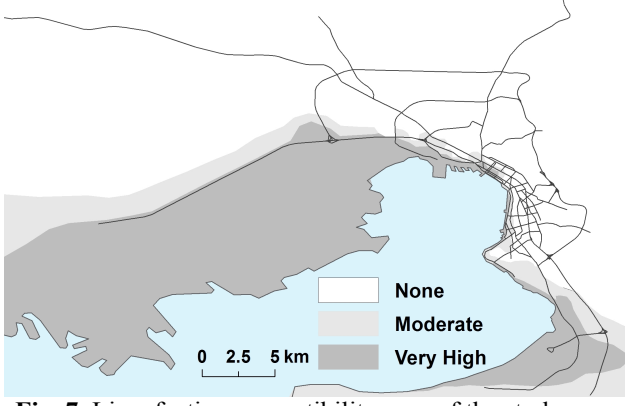

Fig. 7. Liquefaction susceptibility map of the study area according to HAZUS classification. Lines represent the main edges of the road network (based on Pitilakis et al., 2013).

The nodes of the network are subdivided into 15 External nodes, 127 TAZs centroids and 452 simple Intersections and, 495 edges are two-ways roads, while 179 are one-way roads. In particular, one-way roads have been considered as single directed edges, and two-ways roads are associated with a second edge (i.e., one edge for each direction). This is specifically relevant for the analysis of general traffic (not only for emergency use). Further information for roadway edges include the road width, road class (minor, principal or highway), distance from buildings, existence of buildings in one or two sides of the edge, capacity, number of ways and free flow speed. The distance from buildings is based on data extracted through remote sensing techniques (Tenerelli and Crowley, 2013) and on information from previous study (Argyroudis 2010).

The building stock is also included in the analysis in order to estimate the road blockages due to collapses of adjacent buildings. The building inventory covers the entire municipality of Thessaloniki; it comprises 2,893 building blocks with 27,738 buildings, the majority of which (25,639) are reinforced concrete (RC) buildings, while the rest (2,099) are masonry buildings. The inventory includes information about material, code level, number of storey, structural type and volume for each building. The database is based on previous project results (Kappos et al., 2008) and has been expanded within SYNER-G project using remote sensing techniques (Tenerelli and Crowley, 2013).

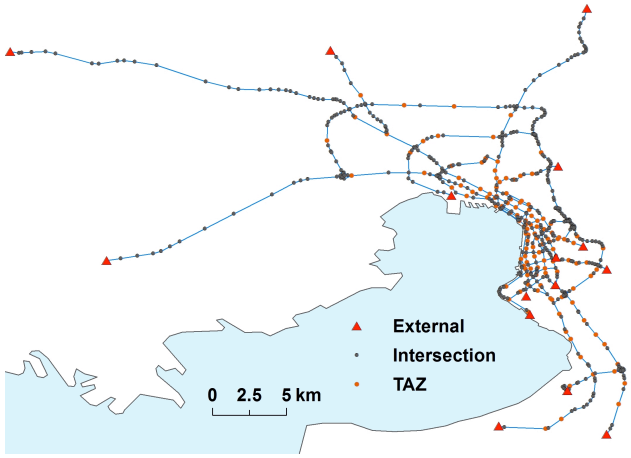

Fig. 8. Road network of Thessaloniki case study.

4.3 Physical vulnerability models

Edges are assumed to be the only vulnerable components in RDN. In this particular application they are classified into road pavements and bridges, with fragility models expressed in terms of PGD due to liquefaction and PGA for ground shaking, respectively. The fragility curves provided in HAZUS (FEMA, 2003) are used for the road pavements of two traffic lanes. These functions are the only available in the literature and they are assumed adequate for the damage assessment in this application.

Analytical fragility curves were constructed for 22 bridges, out of the 60 that are located in the study area, for which detailed construction drawings were made available

by the competent authorities. The most appropriate among these fragility curves are assigned to the remaining bridges on the basis of their structural characteristics. They are classified based on the number of spans, deck continuity, deck-pier connection, transverse translation at the abutments, year of construction and pier type (Tsionis and Fardis 2014; Pitilakis and Argyroudis, 2013). Peak ground acceleration is adopted as intensity measure and two damage states, namely yielding of the piers and ultimate condition of the piers and the bearings, are considered. A bridge in ultimate state is not functional and the corresponding edge is removed from the network (broken). In case of an overpass in ultimate state, the procedure described in 3.3.4 is followed. The obtained fragility curves show that older bridges, designed with low seismic code (i.e., built before 1992, when advanced seismic code for bridges has been introduced in Greece), are likely to experience damage for low to medium levels of earthquake excitation. On the other hand, modern bridges are markedly less vulnerable (Figure 9).

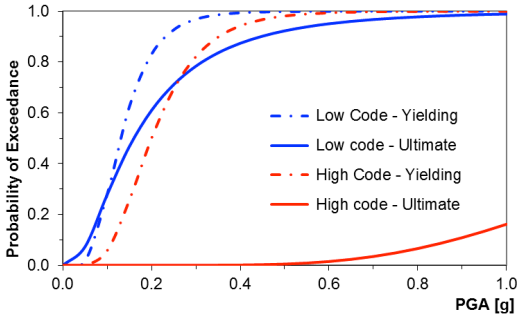

Fig. 9. Fragility curves for a bridge with the deck supported on bearings, constructed in 1985 (low seismic code) and a bridge with monolithic deck-pier connection, constructed in 2000 (high seismic code).

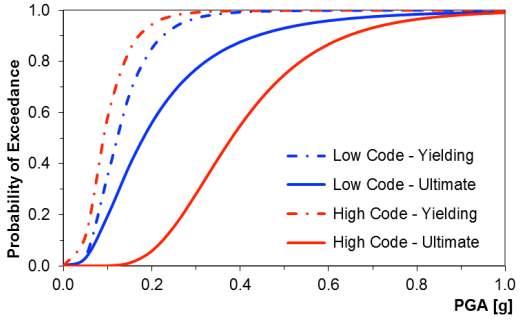

Fig. 10. Fragility curves for low-rise wall-frame buildings designed with low and high-level seismic code.

Analytical fragility curves for RC buildings (Fardis et al., 2012) and masonry buildings (Karantoni et al., 2012) are applied. RC buildings are classified based on the structural system, level of seismic design and height. Masonry buildings are classified to low and mid-rise with rigid or flexible floors buildings. Peak ground acceleration is adopted as intensity measure and two damage grades, namely yielding and ultimate, are considered. An example of the fragility curves for wall-frame buildings are shown in Figure 10, where the effect of design codes is evident (Pitilakis and Argyroudis, 2013).

For the estimation of debris extent due to collapsed buildings the model B in Figure 2 is applied. This is considered more appropriate for continuous building facades, a typical pattern in the study area, where buildings are in contact. For the application of the model it is assumed that W=15m, $E[k_v]$=50%, $E[c]$=45^0 with coefficient of variation $V[k_v]=V[c]$= 30%.

5 RESULTS

The analysis results as obtained from a plain MCS are presented in the following figures with reference to the 'closed' network (FL_2) due to building and overpass collapses as well as direct damage to pavements and bridges. In practice, the network is analysed for each sampled event and the results are aggregated all over the sampled events, in order to numerically obtain the marginal distribution of performance losses (Equation 1). In this way, all the characteristics of each event (e.g., spatial correlations) are accounted for and preserved for the systemic analysis.

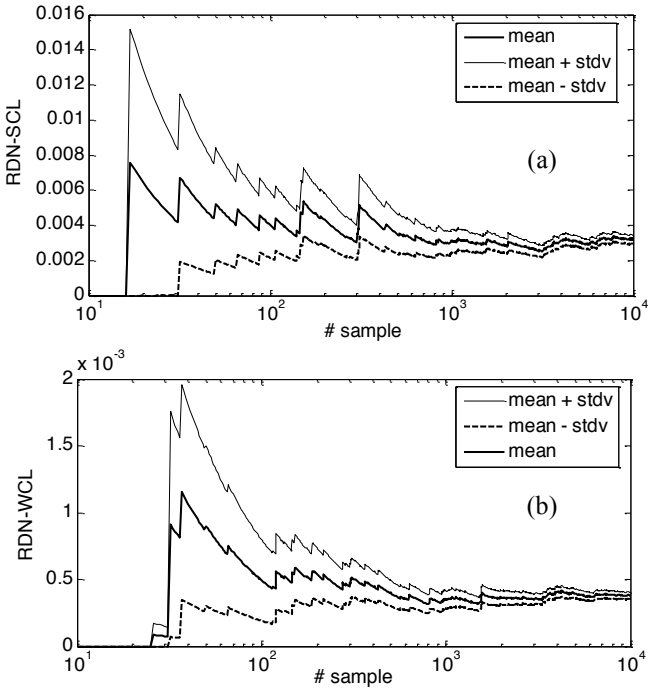

Fig. 11. Moving average μ, μ+σ$_\mu$, μ-σ$_\mu$ curves for SCL (a) and WCL (b).

Figure 11 shows the cumulative moving average (mean value on all previous runs, as a function of runs) for SCL and WCL, as well as confidence bounds (+/- standard deviation of the mean, *stdv*, for the two PI's). Note that this average is computed over earthquake samples (mean value per event), and not over time (i.e., each run gives a time-independent snapshot of the situation just after the event,

without any notion of evolution over time). The stabilization of the estimate of the mean values is used here as main convergence criterion. After few thousands runs, the moving averages for both PIs seem to reach reasonably stable values and thus, the analysis is terminated after 10,000 runs. Figure 11 also indicates that the expected value of connectivity loss (i.e., existence of a path between two TAZs) given the occurrence of an earthquake is higher for WCL than for SCL. The discontinuities present in the plots are located in correspondence of simulation runs/samples in which significant loss in performance is recorded (so that the mean PI decreases) and the number of runs until then is not large enough to have stable mean values. For both PIs, significant loss in performance occurs when at least one TAZ node is not connected, leading SCL and WCL to yield values greater than 0.

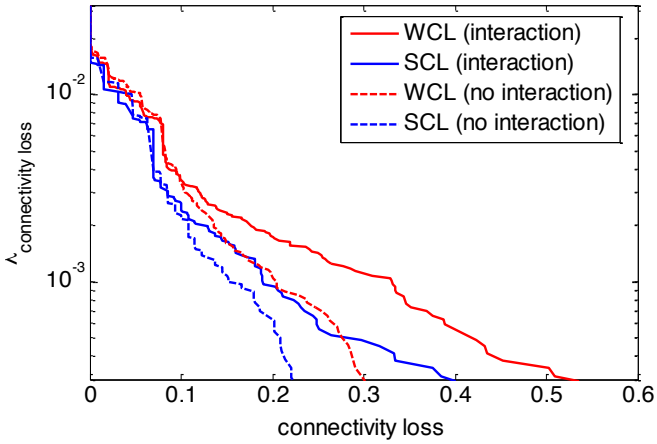

Fig. 12. MAF curves for simple (SCL) and weighted (WCL) connectivity loss with and without interaction with building collapses.

Figure 12 shows the mean annual frequency (MAF) of exceedance curves for SCL and WCL, i.e., the performance curves. WCL takes into account not only the existence of a path between two TAZs, but also the travel time increase due to damage in RDN components, therefore its values of exceedance are higher than the SCL. The same figure compares the estimated MAF of exceedance curves for SCL and WCL when the road blockage due to collapsed building is not considered in the analysis. The interaction with building collapses has a significant impact, especially for low annual rates, that is, smaller than λ=0.002 (corresponding to return periods T_R of SCL and WCL higher than 500 years). As an example the WCL is increased from 20% to 33% for λ=0.001 (T_R=1000 years) when the building collapses are included in the analysis. For lower return periods that correspond to less severe events, building collapses are limited or inexistent therefore the curves practically coincide. Note that small differences are expected due to the simulation-based scheme that is here adopted.

Figure 13 and 14 show the level of correlation between the WCL and road blockages due to building collapses and damages in bridges and road segments, respectively. This correlation analysis is performed in order to identify components (either internal to RDN or external to it) that specifically tend to control PIs, and thus, that can be considered critical for the performance of RDN. Relatively higher correlations are found for RDN edges blocked by building collapse, demonstrating the importance of this failure mechanism for RDN analysis. In particular, the most correlated blocked roads are mainly in the historical centre of the city, where the vulnerability of buildings (mostly built with the oldest seismic code in Greece) is higher and the road-to-building distances are shorter. Several road segments in the city centre and the southeast part of the study area present a medium correlation due to building collapses. The high correlation of broken edges (Figure 14) near the coast is instead related to ground failure due to liquefaction, while the other broken edges are mainly damaged bridges. The latter is attributed to highly vulnerable bridges (i.e. older structures with poor seismic design).

6 CONCLUSIONS

The implementation of the analysis of a road networks under the effect of seismic events is presented. In particular, it is developed a generalized and comprehensive model that accounts for seismic statistical characterization of seismic input acting on the components, intra-dependencies among the network components, and inter-dependencies with external systems, as the built environment. The computational model is demonstrated and tested through an application to the main road network of Thessaloniki (Greece). All sources of aleatory uncertainty are formally treated within a probabilistic framework, leading to a fully probabilistic risk assessment.

This analysis, as well as any analysis for extended systems, requires the modeling of spatial correlations (through intra-event residuals) and multiple intensity measures. Indeed, spatial correlations of intensity measures (and consequently of damages) within the network may play a relevant role in its performance. To account for this, single seismic scenarios are firstly analyzed, and then the results of the systemic analysis are statistically combined.

Through the application to the road network, it is shown that its performance (at least at urban level) is highly controlled by inter-dependencies. Indeed, such interactive effects strongly modify the performance curves (exceedance probability of loss in performance), in particular for high levels of performance loss corresponding to small mean annual rates (i.e., high return periods). This means that an unbiased systemic analysis should include a complex system-of-system analysis, including all the systems that may potentially induce non-functionalities to the road network. In particular, in the urban context of the application, it is found that building collapses seem to be

the most important mechanism of performance loss for the road network.

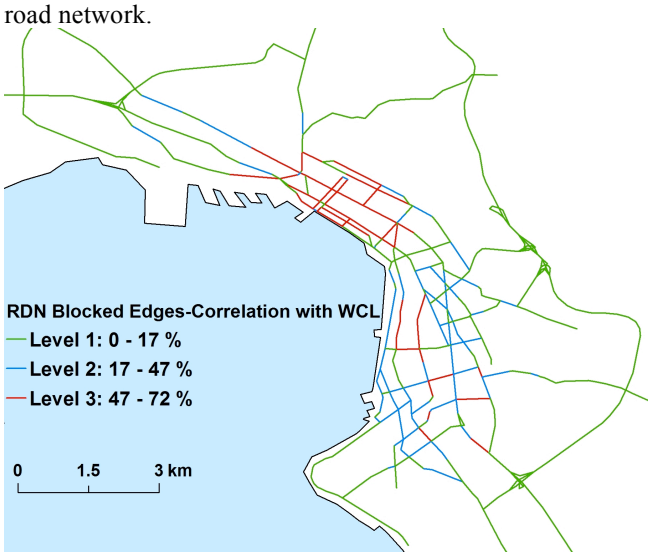

Fig. 13. Correlation of blocked by buildings edges to road network connectivity (PI=WCL).

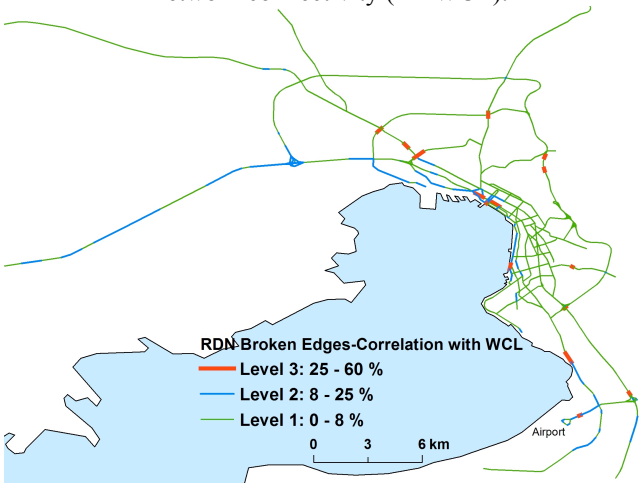

Fig.14. Correlation of broken edges (damaged bridges and road segments) to road network connectivity (PI=WCL).

The need of accounting for and statistically combining single scenarios instead of using aggregated hazard and the need of modeling a large set of interacting components (within and external to the studied network), complicates the definition of simple rules for design requirements and mitigation needed to meet acceptable risk levels, at least as commonly implemented with seismic codes or 'risk-targeted' approaches (EC8, 2004; Douglas et al., 2013). The presented framework identifies the most critical components for the network performance and it quantifies its performance under seismic conditions. Thus, once desired levels of performance are defined, the presented framework can be used to 'translate' such levels into acceptable failure probabilities of single components within the system and to evaluate different mitigation schemes. However, the selection of target levels of performance is not only a technical civil engineering issue and should ideally involve input from the wider community (e.g., decision makers) as to what level of seismic risk is acceptable for each given network.

Of course, many sources of epistemic uncertainties are inherent in the analysis. Such sources of uncertainty are present in all the steps of the analysis, from seismic hazard and spatial correlation models, to fragility and functionality assessments of each component, and from network specifications to network analysis. In this context, we stress that specific sensitivity analysis will be required in future analyses, in order to constrain the impact of such uncertainties in systemic analyses.

ACKNOWLEDGMENTS

This work has been developed in the framework of the research project SYNER-G funded from the European Community's 7th Framework Program under grant 244061. The authors would also like to acknowledge Francesco Cavalieri and Paolo Franchin from University of Rome La Sapienza for their contribution and support to the implementation of the adopted prototype software.

REFERENCES

Adachi, T. (2007), Impact of cascading failures on performance assessment of civil infrastructure systems. *Dissertation,* School of Civil and Environmental Engineering, Georgia Institute of Technology.

Adachi, T. & Ellingwood, B.R. (2009), Serviceability assessment of a municipal water system under spatially correlated seismic intensities. *Computer-Aided Civil and Infrastructure Engineering, **24***, 237-248

Akkar, S. & Bommer, J.J. (2010), Empirical equations for the prediction of PGA, PGV and spectral accelerations in Europe, the Mediterranean region and the Middle East. *Seismological Research Letters*, **812**, 195-206.

Argyroudis, S. & Kaynia, A.M. (2014), Chapter 10, in: K. Pitilakis et al. (eds) *SYNER-G: Typology definition and fragility functions for physical elements at seismic risk*, Springer, Netherlands.

Argyroudis, S. (2010), Contribution to seismic vulnerability and risk of transportation networks in urban environment. *Dissertation*, Aristotle University of Thessaloniki, Greece (in greek).

Banerjee, S. & Shinozuka, M. (2005), Nonlinear static procedure for seismic vulnerability assessment of bridges. *Computer-Aided Civil and Infrastructure Engineering*, **22**(4), 293-305.

Bardet, J.P. (2004), Preliminary observations of the Niigata-ken Chuetsu, Japan, Earthquake of October 23, 2004. *GEER Association Report No. GEER-009*.

Cavalieri, F., Franchin, P., Gehl, P. & Khazai, B. (2012), Quantitative assessment of social losses based on physical

damage and interaction with infrastructural systems. *Earthquake Engineering and Structural Dynamics*, **41**(11), 1569-1589.

Chang, L., Elnashai, A.S., Spencer, B.F., Song, J. & Ouyang, Y. (2011), Transportation system modeling and applications in earthquake engineering. *Report 10-03, Mid-America Earthquake (MAE) Center*.

Cho, S., Gordon, P., Moore, J., Richardson, H., Shinozuka, M. & Chang, S. (2001), Integrating transportation network and regional economic models to estimate the costs of a large urban earthquake. *Journal of Regional Science*, **41**(1), 39-65.

Cornell, C. & Krawinkler, H. (2000), Progress and challanges in seismic performance assessment. *PEER Center News,* **3**(2).

Crowley, H., Bommer, J.J. & Stafford, P.J. (2008), Recent developments in the treatment of ground-motion variability in earthquake loss models. *Journal of Earthquake Engineering,* **12**(S2), 71-80

Dolce, M., Giovinazzi, S., Iervolino, I., Nigro, E. & Tang, A. (2009), Emergency management for lifelines and rapid response after L'Aquila earthquake. Progettazione Sismica. *Seismic Design Journal,* **3**, November, IUSS PRESS Editor, ISSN 1973-7432

Douglas, J., Ulrich, T. & Negulescu, K. (2013), Risk-targeted seismic design maps for mainland France. *Natural Hazards*, **65**(3), 1999-2013.

Dudenhoeffer, P. & Permann, D. (2006), Critical infrastructure interdependency modeling: a survey of US and international research. *Report INL/EXT-06-11464*, Idaho National Laboratory.

Duenas-Osorio, L., & Rojo, J. (2010), Reliability assessment of lifeline systems with radial topology. *Computer-Aided Civil and Infrastructure Engineering*, **26**, 111-128.

Eurocode 8, EC8 (2004), Design of structures for earthquake resistance. *European Committee for Standardisation*. The European Standard EN 1998-1.

Esposito, S., Iervolino, I., d'Onorio A., Cavalieri, F., Franchin, P. (2014), Simulation-based seismic risk assessment of gas distribution networks *Computer-Aided Civil and Infrastructure Engineering*, accepted.

Esposito, S. & Iervolino, I. (2011), PGA and PGV spatial correlation models based on European multi-event datasets. *Bulletin of the Seismological Society of America*, **101**(5), 2532-2541.

Fardis, M.N., Papailia, A. & Tsionis, G. (2012), Seismic fragility of RC framed and wall-frame buildings designed to the EN-Eurocodes. *Bulletin of Earthquake Engineering*, **10**(6), 1767-1793.

FEMA (2003), HAZUS-MH Technical Manual. Federal Emergency Management Agency, Washington DC, USA.

Franchin, P. & Cavalieri, P. (2013), Seismic vulnerability of a complex interconnected infrastructure. In: Tesfamariam, S. & Goda, K. (eds) *Handbook of seismic risk analysis and management of civil infrastructure systems*, Woodhead Publishing Ltd, Cambridge, UK.

Franchin, P. & Pinto, P.E. (2009), Allowing traffic over mainshock-damaged bridges. *Journal of Earthquake Engineering*, **13**, 585-599.

Franchin, P. (ed) (2013), Methodology for systemic seismic vulnerability assessment of buildings, infrastructures, networks and socio-economic impacts, *SYNER-G Reference Report 1*. Publications Office of the European Union, doi: 10.2788/69238, pp. 164.

Franchin, P., Lupoi, A., & Pinto, P.E. (2006), On the role of road network in reducing human losses after earthquakes. *Journal of Earthquake Engineering*, **10**(2), 195-206.

Ghosh, J. & Padgett, J.E. (2010), Aging considerations in the development of time-dependent seismic fragility curves. *Journal of Structural Engineering*, **136**(12), 1497-1511.

Giardini, D., et al., (2013) Seismic Hazard Harmonization in Europe (SHARE). *Online Data Resource*, doi: 10.12686/SED-00000001-SHARE.

Goretti, A. & Sarli, V. (2006), Road network and damaged buildings in urban areas: short and long-term interaction. *Bulletin of Earthquake Engineering*, **4**,159-175.

Grunthal, G., Thieken, A., Schwarz, J., Radtke, K., Smolka, A. & Merz, B. (2006), Comparative risk assessments for the city of Cologne-storms, floods, earthquakes. *Natural Hazards*, **38**(1-2), 21-44.

Hancilar, U. & Taucer, F. (eds) (2013), Guidelines for typology definition of European physical assets for earthquake risk assessment. *SYNER-G Reference Report 2*, Publications Office of the European Union, ISBN 978-92-79-28973-6.

Harr, M.E. (1987), *Reliability-based design in civil engineering*. Mc Graw-Hill, New York, NY.

Iervolino, I., Giorgio, M., Galasso, C., & Manfredi, G. (2010), Conditional hazard maps for secondary intensity measures. *Bulletin of the Seismological Society of America,* **100**(6), 3312-3319.

Jayaram, N. & Baker, J. (2009), Correlation model of spatially distributed ground motion intensities. *Earthquake Engineering and Structural Dynamics,* **38**, 1687-1708.

Kappos, A.J., Panagopoulos, G., Penelis, G. (2008), Development of a seismic damage and loss scenario for contemporary and historical buildings in Thessaloniki, Greece. *Soil Dynamics and Earthquake Engineering*, **28**, 836-850.

Karaca, E. (2005), Regional earthquake loss estimation: role of transportation network, sensitivity and uncertainty, and risk mitigation. *Dissertation*, MIT, Cambridge, MA.

Karantoni, F., Lyrantzaki, F., Tsionis, G. & Fardis, M.N. (2012), Seismic fragility functions of stone masonry buildings, In *Proceedings 15th World Conference on Earthquake Engineering*, 24-28 September, Lisbon.

Kiremidjian, A., Moore, J., Fan, Y., Yazlali, O., Basöz, N.I. & Williams, M. (2007), Seismic risk assessment of

transportation network systems. *Journal of Earthquake Engineering*, **11**, 371-382.

Modaressi, H., Desramaut, N. & Gehl, P. (2014), Chapter 5, in: K. Pitilakis et al. (eds). *SYNER-G: Systemic seismic vulnerability and risk assessment of complex urban, utility, lifeline systems and critical facilities. Methodology and applications*, Springer, Netherlands.

National Institute of Standards and Technology (NIST) (1996), The January 17, 1995 Hyogoken-Nanbu (Kobe) earthquake. Performance of structures, lifelines and fire protection systems. *NIST Special Publication 901*, July.

Nielson, B.G. & DesRoches, R. (2007), Seismic fragility methodology for highway bridges using a component level approach, *Earthquake Engineering and Structural Dynamics*, **36**, 823-839.

Nuti, C. & Vanzi, I. (1998), Assessment of post-earthquake availability of hospital system and upgrading strategies, *Earthquake Engineering and Structural Dynamics*, **27**, 1403-1423.

Papazachos, B.C. & Papazachou, C. (1997), *The earthquakes of Greece*, Ziti Publications, Thessaloniki.

Pate-Cornell ME (1996) Uncertainties in risk analysis: six levels of treatment. *Reliability Engineering & System Safety*, **54**, 95-111.

Perkins, J., Chuaqui, B., Wyatt, E. (1997), Riding out future quakes - Pre-earthquake planning for post-earthquake transportation system recovery in the San Francisco Bay region. Publication of the Association of Bay Area Governments, Oakland, CA, October.

Pitilakis, K. & Argroudis, S. (eds) (2013), Systemic seismic vulnerability and loss assessment: Validation studies. *SYNER-G Reference Report 6*, Publications Office of the European Union, ISBN 978-92-79-30840-6.

Pitilakis, K., Riga, E. & Anastasiadis, A. (2013), New design spectra in Eurocode 8 and application to the seismic risk of Thessaloniki, Greece. *Invited Lecture in International Conference on Earthquake Geotechnical Engineering*: *From Case History to Practice*, Istanbul, Turkey, 17-19 June 2013.

Pitilakis, K.D, Karapetrou, S.T., Fotopoulou, S.D. (2014), Consideration of aging and SSI effects on seismic vulnerability assessment of RC buildings. *Bulletin of Earthquake Engineering,* **12**, 1755-1776.

Poljanšek, K., Bono, F. & Gutiérrez, E. (2012), Seismic risk assessment of interdependent critical in-frastructure systems: The case of European gas and electricity networks. *Earthquake Engineering and Structural Dynamics*, **41**(1).

Rinaldi, S.M., Peerenboom, J.P. & Kelly, T.K. (2001), Identifying, understanding and analyzing critical infrastructure interdependencies. *IEEE Control Systems Magazine*, **21**(6), 11-25.

Schweier, C. & Markus, M. (2006) Classification of collapsed buildings for fast damage and loss assessment. *Bulletin of Earthquake Engineering*, **4**(2), 177-192.

Selva, J. (2013), Long-term multi-risk assessment: statistical treatment of interaction among risks, *Natural Hazards,* **67**(2), 701-722.

Selva, J., Argyroudis, S. & Pitilakis, K. (2013), Impact on loss/risk assessments of inter-model variability in vulnerability analysis, *Natural Hazards*, 67(2), 723-746.

Song, J. & Ok, S-Y. (2010), Multi-scale system reliability analysis of lifeline networks under earthquake hazards. *Earthquake Engineering and Structural Dynamics*, **39**, 259-279.

SYNER-G (2013), Systemic seismic vulnerability and risk analysis for buildgins, lifeline networks and infrastructures safety gain. *European Collaborative research project* (FP7/2007-2013). http://www.syner-g.eu.

Tenerelli, P. & Crowley, H. (eds) (2013), Development of inventory datasets through remote sensing and direct observation data for earthquake loss estimation. *SYNER-G Reference Report 3*. Publications Office of the European Union, doi: 10.2788/86322, pp. 82.

Tang, C., Zhu, J. & Qi, X. (2011), Landslide hazard assessment of the 2008 Wenchuan earthquake: a case study in Beichuan. *Canadian Geotechnical Journal*, **48**, 128-145.

Tsionis, G. & Fardis, M.N. (2014), Chapter 9, in: K. Pitilakis et al., (eds) *SYNER-G: Typology definition and fragility functions for physical elements at seismic risk*, Springer, Netherlands.

Tung, P.H. (2004), Road vulnerability assessment for earthquakes. A case study of Lalitpur, Kathmandu - Nepal, Master Thesis, International Institute for Geo-Information Science and Earth Observation, Enschede, The Netherlands.

Veneziano, D., Sussman, J., Gupta, U. & Kunnumkal, S.M. (2002), Earthquake loss under limited transportation capacity: assessment, sensitivity and remediation. In *Proceedings of 7th USNCEE*, Boston, MA, USA.

Weatherill, G., Esposito, S., Iervolino, I., Franchin, P. and Cavalieri, F. (2014), Chapter 3, in: K. Pitilakis et al. (eds). *SYNER-G: Systemic seismic vulnerability and risk assessment of complex urban, utility, lifeline systems and critical facilities. Methodology and applications*. Springer, Netherlands.

Werner, S.D., Taylor, C.E., Cho, S., Lavoie, J-P., Huyck, C., Eitzel, C., Chung, H. & Eguchi, R.T. (2006), REDARS 2: Methodology and software for seismic risk analysis of highway systems. *MCEER-06-SP08*.

Woo, G. (1999) The mathematics of natural catastrophes. Imperial College Press, London.

Youd, T.L. & Perkins, D.M. (1978), Mapping of liquefaction induced ground failure potential. *Journal of Geotechnical Engineering Division*, ASCE **1044**, 433-466.

Zhou, Y., Murachi, Y., Kim, S.H. & Shinozuka, M. (2004), Seismic risk assessment of retrofitted transportation systems. In *Proceedings of 13th World Conference on Earthquake Engineering, Vancouver*, BC, Canada.